Electronic structure, phase stability, and chemical bonding in Th_2Al and Th_2AlH_4

P. Vajeeston,[1,*] R. Vidya,[1] P. Ravindran,[1] H. Fjellvåg,[1,2] A. Kjekshus,[1] and A. Skjeltorp[2]
[1]*Department of Chemistry, University of Oslo, Box 1033, Blindern, N-0315, Oslo, Norway*
[2]*Institute for Energy Technology, P.O. Box 40, Kjeller, N-2007, Norway*
(Received 16 August 2001; published 16 January 2002)

We present the results of a theoretical investigation on the electronic structure, bonding nature, and ground-state properties of Th_2Al and Th_2AlH_4 using generalized-gradient-corrected first-principles full-potential density-functional calculations. Th_2AlH_4 has been reported to violate the ''2-Å rule'' for H-H separation in hydrides. From our total-energy as well as force-minimization calculations, we found a shortest H-H separation of 1.95 Å in accordance with recent high-resolution powder neutron-diffraction experiments. When the Th_2Al matrix is hydrogenated, the volume expansion is highly anisotropic, which is quite opposite to other hydrides having the same crystal structure. The bonding nature of these materials is analyzed in terms of density of states, crystal-orbital Hamiltonian population, and valence-charge-density analyses. Our calculation predicts a different nature of the bonding between the H atoms along *a* and *c*. The strongest bonding in Th_2AlH_4 is between Th and H along *c* which form dumbbell-shaped H-Th-H subunits. Due to this strong covalent interaction there is a very small amount of electrons present between the H atoms along *c*. This reduces the repulsive interaction between the H atoms along *c* and explains why Th_2AlH_4 has a shorter H-H separation than most other metal hydrides. The large difference in the interatomic distances between the interstitial regions where one can accommodate H in the *ac* and *ab* planes along with the strong covalent interaction between Th and H are the main reasons for highly anisotropic volume expansion on hydrogenation of Th_2Al.

DOI: 10.1103/PhysRevB.65.075101 PACS number(s): 71.15.Nc, 71.20.−b, 81.05.Je

I. INTRODUCTION

Hydrides of intermetallics have been extensively studied because of their applications in rechargeable batteries. Unfortunately, most metals that absorb large amounts of hydrogen are heavy and/or expensive.[1] Consequently, there is a constant search for hydrides that may be suitable for practical applications. First of all, it is very important to understand how crystal structural evolution takes place in the course of hydrogenation. Numerous studies have been done to explain observed stabilities, stoichiometries, and preferred H sites in hydrides of metallic and intermetallic compounds. Structural studies of hydrides have provided empirical rules[2] that can be used to predict the stability of the H sublattice in a given metal configuration. A survey of stable hydrides shows that the H-H distance does not go below 2.1 Å (the ''2-Å rule'') with a minimum ''radius'' of 0.4 Å for the intersite to be used for the accommodation of H. These rules have been used to predict new hydrides whose existence later has been verified experimentally.[1–3]

The review of Yvon and Fischer[4] states that Th_2AlH_4 (Ref. 5) and K_2ReH_9 (Refs. 4 and 6) violate the 2-Å rule, the shortest H-H separation being 1.79 and 1.87, respectively. K_2ReH_9 is classified among complex transition-metal hydrides, which comprise highly covalent solids with nonmetallic properties. Th_2AlH_4, on the other hand, has metallic character.

Th_2Al[7] together with Zr_2Fe, Zr_2Co, and Zr_2Ni crystallize in the $CuAl_2$-type structure, whereas their hydrides form rather different crystal structures. Zr_2Fe and Zr_2Co form the isostructural deuterides Zr_2MD_5 (M=Fe,Co)[8] with a change in symmetry from $I4/mcm$ to $P4/ncc$ on deuteration. Th_2AlH_4 (Refs. 5 and 9) and $Zr_2NiH_{4.74}$ (Ref. 10) are formed without any change in the symmetry from their parent structures. Th_2AlH_4 belongs to the exclusive class which does not obey the 2-Å rule. The lattice expansion along *a* and *c* has proved to be highly anisotropic on hydrogenation of Th_2Al. In order to shed light on this effect we need theoretical understanding about the bonding nature in this compound. Further, the understanding of the lattice expansion and distortion during hydrogenation will be important for the evaluation of stability of the hydride. So, we have made a detailed study of Th_2Al and Th_2AlH_4 by first-principles calculations.

Two different powder neutron-diffraction (PND) studies of Th_2AlH_4 give different H-H separations, viz., the older[5] value is 1.79 Å and the more recent[9] value is 1.97 Å. So one aim of this study has been to solve this discrepancy. In principle, the stability of hydrides can be evaluated directly from a theoretical study of the total energy. However, owing to the complexity of the structure of transition-metal hydrides, to our best knowledge, no reliable theoretical heat of formation has hitherto been reported.[11] Nakamura *et al.*[11] were the first to calculate heat of formation for this type of hydrides. However, these authors obtained a positive and unrealistically large heat of formation even for stable La-Ni-based hydrides, except for $La_2Ni_{10}H_{14}$.[12–14] This unfavorable result clearly indicates that local relaxation of the metal atoms surrounding the hydrogens must be included in the calculations in order to predict the structural stability parameters. Hence, our calculations take into account local relaxation by optimizing the atom positions globally.

We present the electronic structure of Th_2Al and Th_2AlH_4, obtained by the full-potential linearized-augmented plane-wave (FPLAPW) method. A central feature of the paper is the evaluation of the electronic structure and bonding characteristics on introduction of H into the Th_2Al matrix. In addition to regular band-structure data, we also

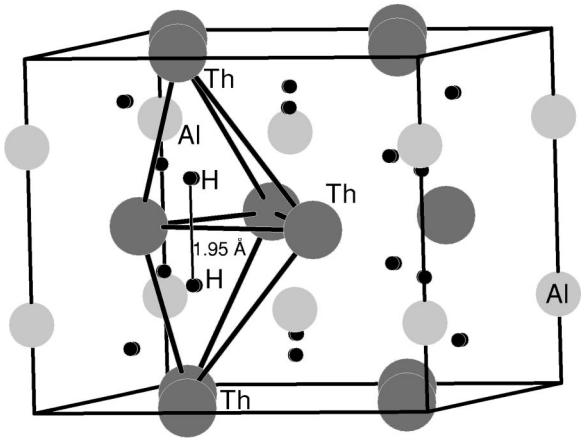

FIG. 1. The crystal structure of Th_2AlH_4. Five Th in face-sharing tetrahedral (bipyramidal) configuration surround two hydrogen. Legends to the different kinds of atoms are given on the illustrations.

provide crystal-orbital Hamiltonian population (COHP) (Refs. 15 and 16) results to illustrate the chemical bonding in more detail.

This paper is organized as follows. Details about the involved structure and computational method are described in Sec. II. Section III gives the results of the calculations and comparisons with the experimental findings. Conclusions are briefly summarized in Sec. IV.

II. STRUCTURAL DETAILS

Th_2Al and Th_2AlH_4 crystallize in space group $I4/mcm$ with the lattice parameters $a=7.618$, $c=5.862$ Å for Th_2Al (Ref. 17) and $a=7.626$, $c=6.515$ Å for Th_2AlH_4.[9] The crystal structure of Th_2AlH_4 is illustrated in Fig. 1. The crystal structure of Th_2Al contains four crystallographically different interstitial sites, which are the suitable sites for hydrogen accommodation, 16*l* and 4*b* each coordinates to four Th, 32*m* coordinates to three Th and one Al, and 16*k* coordinates to two Th, and two Al. Each 16*l*-based intersite tetrahedron shares a common face with another 16*l*-based tetrahedron, whereas the 4*b*-based tetrahedron shares each of its four faces with 16*l*-based tetrahedra. Some of the tetrahedral intersites are closely separated owing to the face sharing of the coordination polyhedra. According to the experimental findings,[5,9] the 16*l* sites are fully occupied in Th_2AlD_4, and also the structure is completely ordered.

A. Computational details

In our calculations we use the FPLAPW method in a scalar relativistic version without spin-orbit coupling as embodied in the WIEN97 code.[18] In brief, this is an implementation of density-functional theory (DFT) with different possible approximations for the exchange and correlation potentials, including the generalized-gradient approximation (GGA). The Kohn-Sham equations are solved using a basis of linearized-augmented plane waves.[19] For the exchange and correlation potentials, we used the Perdew and Wang[20] implementation of the GGA. For the potential and charge-density representations, inside the muffin-tin spheres the wave function is expanded in spherical harmonics with $l_{max}=10$, and nonspherical components of the density and potential are included up to $l_{max}=6$. In the interstitial region they are represented by Fourier series and thus they are completely general so that such a scheme is termed a full-potential calculation. In the present calculations we used muffin-tin radii of 2.5, 2.0, and 1.6 a.u. for Th, Al, and H, respectively.

The basis set includes $7s$, $7p$, $6d$, and $5f$ valence and $6s$ and $6p$ semicore states for Th, $3s$ and $3p$ valence and $2p$ semicore states for Al, and $1s$ states for H. These basis functions were supplemented with local orbitals[21] for additional flexibility to the representation of the semicore states and for generalization of the linearization errors. We have included the local orbitals for Th-$6s$, Th-$6p$, and Al-$2p$ semicore states. In all our calculations we have used the tetrahedron method on a grid of 102 **k** points in the irreducible part of the hexagonal Brillouin zone,[22] which corresponds to 1000 **k** points in the whole Brillouin zone. The calculations are done at several cell volumes (around the equilibrium volume) for both Th_2Al and Th_2AlH_4 and corresponding total energies are evaluated self-consistently by iteration to an accuracy of 10^{-6} Ry/cell. Similar densities of **k** points were used for the force minimization and c/a optimization calculations.

In order to measure the bond strengths we have computed the COHP,[16] which is adopted in the tight binding linear muffin-tin orbital (TBLMTO-47) package.[23,24] The COHP is the density of states weighted by the corresponding Hamiltonian matrix elements, which if negative indicates a bonding character and if positive indicates an antibonding character. The simplest way to investigate the bonding between two interacting atoms in the solid would be to look at the complete COHP between them, taking all valence orbitals into account. However, it may sometimes be useful to focus on pair contributions of some specific orbitals.

III. RESULT AND DISCUSSION

The H-H separation is one of the most important factors in identifying the potential candidate for hydrogen storage, because if the H-H separation is small one can accommodate more H within a small region. From this point of view, Th_2AlH_4 may be considered as a potential candidate for storing H. To the best of our knowledge no theoretical or experimental attempts have been made to study cohesive properties like heat of formation (ΔH), cohesive energy (E_{coh}), bulk modulus (B_0), and its pressure derivative (B_0') for this compound. Hence, to our best knowledge, this is the first theoretical attempt to study the ground-state properties and bonding in this compound.

A. Structural optimization from total-energy studies

In order to analyze the effect of hydrogenation on the crystal structure of Th_2Al and to verify the discrepancy between the experimentally observed H-H separations, we have optimized the structural parameters for Th_2Al and Th_2AlH_4.

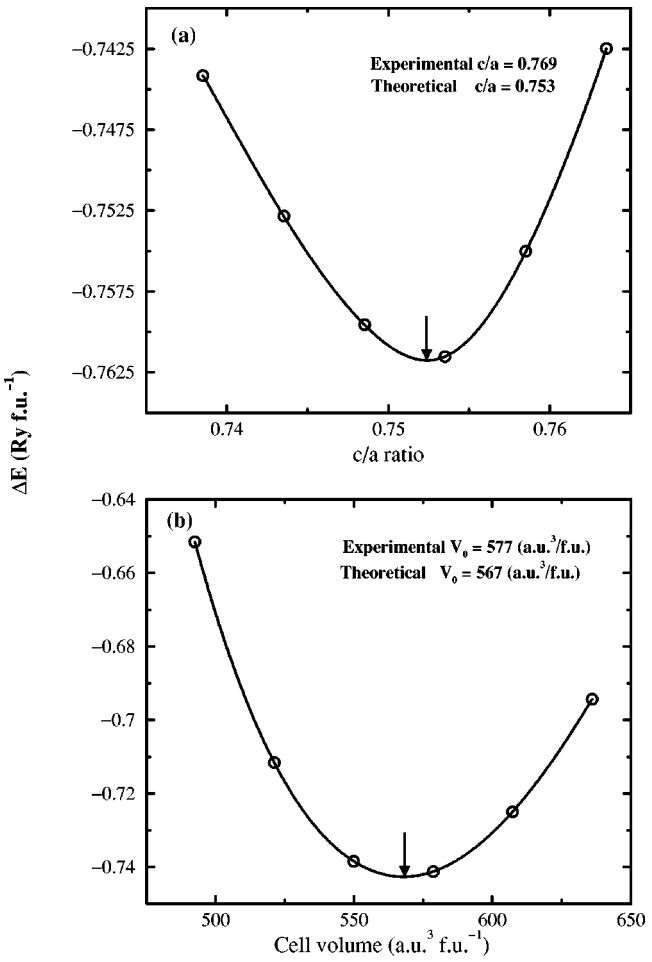

FIG. 2. Total energy (Ry/f.u.) (a) vs c/a and (b) vs unit-cell volume for Th_2Al where $\Delta E = E + 106\,632$. The arrow indicates the theoretical equilibrium.

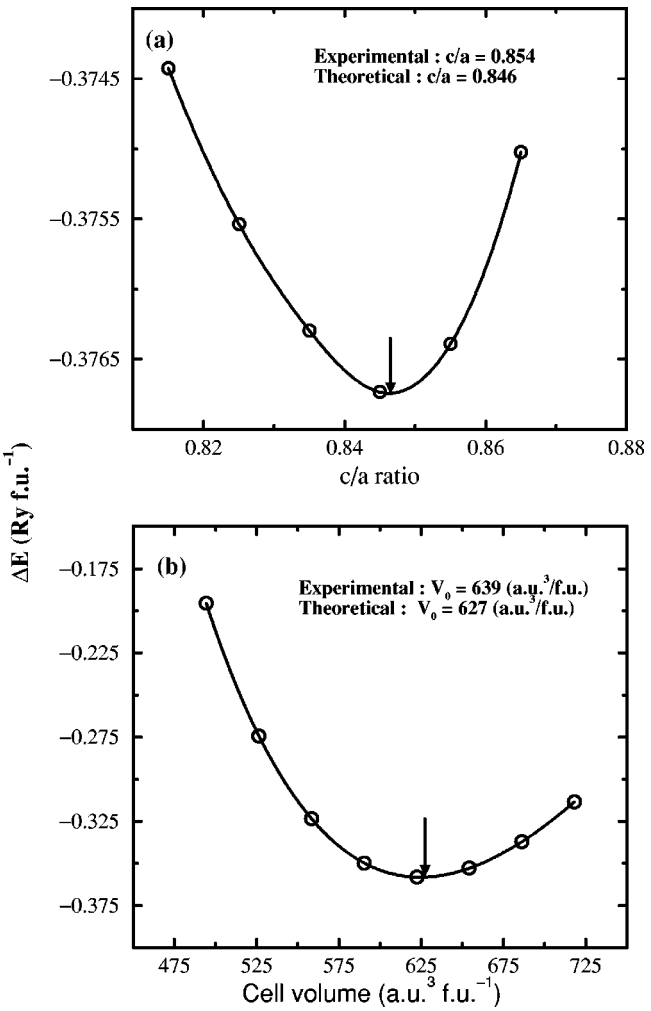

FIG. 3. The total energy (a) vs c/a and (b) vs unit-cell volume for Th_2AlH_4 where $\Delta E = E + 106\,636$. The arrow indicates the theoretical equilibrium.

For this purpose, first we have relaxed the atomic positions globally using the force-minimization technique, by keeping c/a and cell volume (V_0) fixed to experimental values. Then the theoretical equilibrium volume is determined by fixing optimized atomic positions and experimental c/a, and varying the cell volume within $\pm 10\%$ of V_0. Finally the optimized c/a ratio is obtained by a $\pm 2\%$ variation in c/a (in steps of 0.005), while keeping the theoretical equilibrium volume fixed. It is important to note that the experimentally observed lattice parameters are almost equal, while the atomic position for H alone differs between the two experimental results (according to Bergsma *et al.*[5] H coordinates are 0.368, 0.868, and 0.137 whereas Sørby *et al.*[9] give 0.3707, 0.8707, and 0.1512). The total energy vs cell volume and c/a ratio curves for Th_2Al and Th_2AlH_4 are shown in Figs. 2 and 3. From these illustrations it is clear that the equilibrium structural parameters obtained from our theoretical calculations are in very good agreement with those obtained by the recent PND study.[9]

The optimized atomic positions along with the corresponding experimental values are given in Table I. Table II gives calculated lattice parameters and interatomic distances, along with corresponding experimental values for both Th_2Al and Th_2AlH_4. The theoretically estimated equilibrium volume is underestimated by 0.27% for Th_2Al and by 1.8% for Th_2AlH_4. The underestimation of bond length in the present study is partly due to the neglect of the zero-point motion and thermal expansions. The difference between the experimental values may be due to the poor resolution of the 1961 PND data.[5]

B. Cohesive properties

The method of calculation for cohesive properties for intermetallic compounds is well described in Refs. 25–27. The cohesive energy is a measure of the force that binds atoms together in the solid state. The cohesive energy of a system is defined as the sum of the total energy of the constituent atoms at infinite separation minus the total energy of the particular system. This is a fundamental property which has long been the subject of theoretical approaches. The chemical bonding in intermetallic compounds is a mixture of covalent, ionic, and metallic bonding and therefore the cohesive energy cannot be determined reliably from simple models. Thus, first-principles calculations based on DFT

TABLE I. Atomic positions of Th_2Al and Th_2AlH_4.

	Th_2Al			Th_2AlH_4		
	x	*y*	*z*	*x*	*y*	*z*
Th						
Theory	0.1583	0.6583	0.0000	0.1632	0.6632	0.0000
Experiment [a]	0.1588	0.6588	0.0000			
Experiment [b]				0.1656	0.6656	0.0000
Experiment [c]				0.162	0.662	0.0000
Al						
Theory	0.0	0.0	0.25	0.0	0.0	0.25
Experiment [a]	0.0	0.0	0.25			
Experiment [b]				0.0	0.0	0.25
Experiment [c]				0.0	0.0	0.25
H						
Theory				0.3705	0.8705	0.1512
Experiment [b]				0.3707	0.8707	0.1512
Experiment [c]				0.368	0.868	0.137

[a]Reference 17.
[b]Reference 9.
[c]Reference 5.

have become a useful tool to determine the cohesive energy of solids. For the study of phase equilibrium the cohesive energy is more descriptive than the total energy, since the latter includes a large contribution from electronic states that do not play a role in bonding. From our cohesive energy calculations we get $E_{coh}=0.15$ and 0.185 eV/atom for Th_2Al and Th_2AlH_4, respectively, indicating that hydrogenation enhances the bond strength in Th_2Al.

The formation energy (ΔH) is introduced in order to facilitate a comparison of system stability. ΔH is defined as the total-energy difference between the energy of the compound and the weighted sum of the corresponding total energy of the constituents. The present type of calculation is not suitable for handling molecules. In order to have the correct heat of formation of the system one has to calculate the total energy of the compounds and the constituents in the same way (i.e., with same exchange-correlation method, radius, etc.). Patton *et al.*[28] calculated the cohesive energy for an H_2 molecule with different exchange-correlation potentials. We have estimated the total energy of the H_2 molecule in the following way. First we have calculated the atomic total energy for H for the spin-polarized case with the same computational parameters we used in the total-energy calculations for Th_2AlH_4. We have then added the cohesive energy of

TABLE II. Lattice parameters and interatomic distances of Th_2Al and Th_2AlH_4 (except for c/a, all values are in angstrom).

	Th_2Al		Th_2AlH_4		
	Theory	Experiment[a]	Theory	Experiment[b]	Experiment[c]
a	7.602	7.618	7.604	7.626	7.629
c	5.723	5.862	6.433	6.515	6.517
c/*a*	0.753	0.769	0.846	0.854	0.854
Th-H			2.273	2.305	2.387
Th-Al	3.199	3.219	3.269	3.278	3.291
Th-Th	3.403	3.421	3.509	3.571	3.495
Al-H			3.051	3.061	3.072
Al-Al	2.861	2.931	3.216	3.257	3.258
H-H (*ac* plane)			1.945	1.971	1.790
H-H (*ab* plane)			2.344	2.305	2.495

[a]Reference 17.
[b]Reference 9.
[c]Reference 5.

TABLE III. Ground-state properties of Th_2Al and Th_2AlH_4.

Parameters	Th_2Al	Th_2AlH_4
$-\Delta H$(kJ mol^{-1})	60	431
E_{coh} (kJ mol^{-1})	43.42	124.95
$N(E_F)$ (states/Ry cell)	58.42	41.13
B_0 (GPa)	93.42	111.36
B_0'	3.41	3.48

4.540 eV/H_2 given in Ref. 28. This will mimic the total energy for the H_2 molecule as that calculated for the bulk material. ΔH provides information about the stability of Th_2Al towards hydrogenation. The calculated ΔH values for La-Ni-based hydrides[11] were almost twice the experimental[12–14] ΔH. As the linear muffin-tin orbital atomic sphere approximation (LMTO-ASA) method was used in that study, this discrepancy was to be expected because the internal relaxation of the atoms was not taken into account and the interstitial potential is not well represented in the LMTO-ASA method. Therefore, ΔH calculated by using the full-potential method should be more reliable. Our calculated values for E_{coh} and ΔH are given in Table III. Since ΔH is more negative and E_{coh} is higher for Th_2AlH_4 than for Th_2Al, we can conclude that Th_2AlH_4 is more stable than Th_2Al. However, no experimental ΔH values for Th_2Al and Th_2AlH_4 are available, but we note that our calculated ΔH for Th_2AlH_4 [-107 kJ/(mol H)] is close to the experimentally observed values of other Th-based hydrides, like ThH_2 having a ΔH value of -73 kJ/(mol H).[29]

From the self-consistent total-energy calculations for eight different volumes within the range of V/V_0 from 0.75 to 1.10 using a universal model[30] of the equation of state, the bulk modulus and its pressure derivative for Th_2Al and Th_2AlH_4 are evaluated (see Table III). The calculated bulk modulus for Th_2Al is 93.42 GPa and for Th_2AlH_4, 111.36 GPa. The corresponding pressure derivatives of the bulk modulus (B_0') are 3.41 and 3.48, respectively. The enhancement of B_0 for the hydrogenated phase indicates that hydrogen plays an important role in the bonding behavior of Th_2AlH_4. In particular, the hydrogenation enhances the bond strength, and hence the change in volume with hydrostatic pressure decreases on hydrogenation. This conclusion is consistent with the observation made from our calculated heat of formation and cohesive energy for Th_2Al and Th_2AlH_4.

C. Anisotropic behavior

For compounds which maintain the basic structural framework, the occupancy of hydrogen in interstitial sites is determined by its chemical environment (different chemical affinity for the elements in the coordination sphere also results in different occupancy). Although the H atom is small and becomes even smaller by chemical bonding to the host, it may deform and stress the host metal considerably depending upon the chemical environment. Lattice expansion usually of the order of 5% to 30%, often anisotropic, results from hydride formation. The record-large volume expansion observed for the change from $CeRu_2$ to $CeRu_2D_5$ (37%) is due to a hydrogen-induced electron transition as shown by x-ray photoemission spectroscopy measurements.[31] A lattice contraction upon hydrogenation has so far only been observed for $ThNi_2$ to $ThNi_2D_2$ (-2.2%). For most hydrides formed from intermetallic compounds the crystal structure usually changes with a loss of symmetry.[32] In general the symmetry decreases as a function of hydrogen content and increases as a function of temperature. However, on hydrogenation of Th_2Al the symmetry remains unchanged.

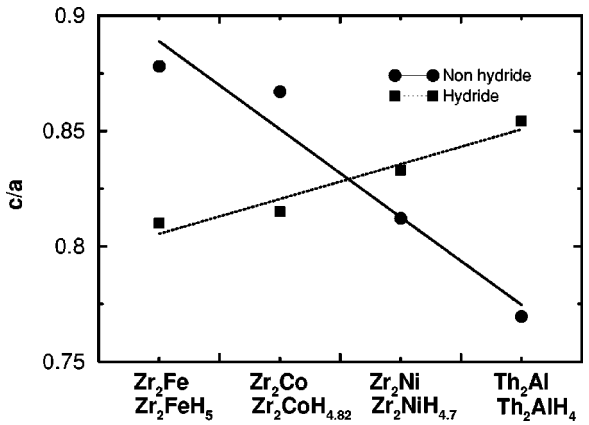

FIG. 4. c/a for $CuAl_2$-type phases and their corresponding hydrides. Lines are guides for the eye.

The volume expansion during hydrogenation of Th_2Al is 12.47% [ΔV/H atom is 10.32 Å^3]. This volume expansion is strongly anisotropic and proceeds predominantly perpendicular to the basal plane of the tetragonal unit cell; $\Delta a/a = 0.026\%$, $\Delta c/c = 12.41\%$. This indicates a relatively flexible atomic arrangement in the [001] direction. In spite of the isostructurality between Th_2Al, Zr_2Fe (hydrated: Zr_2FeH_5),[8] and Zr_2Co (hydrated: $Zr_2CoH_{4.82}$)[33] the Zr-based compounds exhibit a quite opposite anisotropic behavior in that their unit cells expand exclusively along the basal plane. The c/a ratio plays an important role for the structural properties of intermetallic compounds including metal hydrides. For example, in the case of Zr_2Fe,[8] Zr_2Co,[33] Zr_2Ni,[10,34] and Th_2Al c/a is 0.878, 0.867, 0.812, and 0.769, respectively, and for the corresponding hydrides Zr_2FeH_5,[10] $Zr_2CoH_{4.82}$,[10] $Zr_2NiH_{4.74}$,[10] and Th_2AlH_4 c/a is 0.810, 0.815, 0.833, and 0.854, respectively (see Fig. 4). The increase in c/a for $Zr_2CoH_{4.82}$ and Zr_2FeH_5 compared with their corresponding unhydrated parents is smaller than that for other pairs of compounds. On hydrogenation, the increase in the c/a ratio for Th_2Al is considerably larger than for Zr_2Ni, which may be the reason why the former retains its symmetry on hydrogenation. Our calculations describe well the anisotropic changes in the crystal structure on hydrogenation of Th_2Al (see Table II). The c/a ratio increases almost linearly (Fig. 4) on going from Zr_2Fe to Th_2Al whereas the corresponding hydrides show the opposite behavior. Hence, it appears that the systematic variation in c/a plays a major role in deciding the crystal structure for the $CuAl_2$-type hydrides. When $c/a < 0.825$ the symmetry is changed from $I4/mcm$ to $P4/ncc$

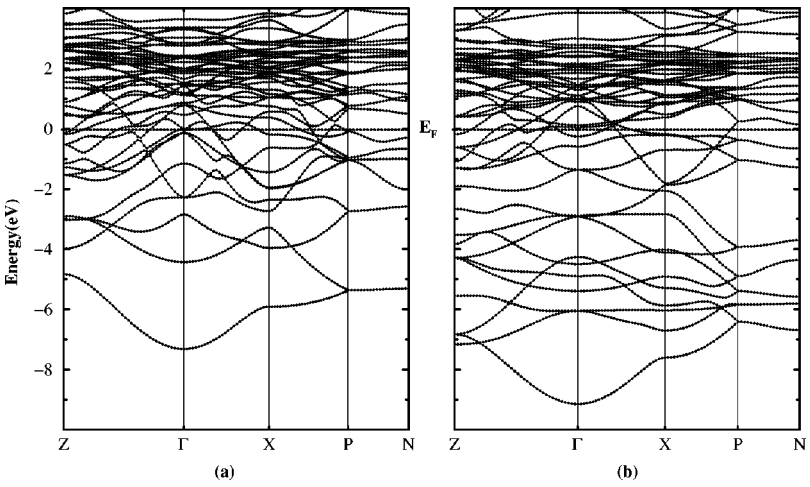

FIG. 5. Electronic band structure of (a) Th_2Al and (b) Th_2AlH_4. The Fermi level is set to zero.

on hydrogenation, whereas when $c/a > 0.825$ the crystal symmetry is apparently not affected.

D. Electronic structure

In order to understand the changes in the electronic bands on hydrogenation of Th_2Al we show the energy-band structure for Th_2Al and Th_2AlH_4 in Fig. 5. The illustrations clearly indicate that inclusion of H in the Th_2Al matrix has a noticeable impact on the band structure, mainly of the valence band (VB). The two lowest-lying broad bands in Fig. 5(a) originate from Al-3s electrons. As the unit cell contains two formula units, eight electrons are additionally introduced when Th_2AlH_4 is formed from Th_2Al. These electrons form four additional bands [Fig. 5(b)], and a large deformation of the band structure is introduced by the hydrogen in the Th_2Al lattice. When these bands become localized, the lowest lying energy band is moved from -7.34 to -9.20 eV, and the character of the latter band is changed from Al-3s to H-1s. The Al-3s bands are located in a wide energy range from -2.8 to -7.34 eV in Th_2Al and are in a narrow energy range from -2.5 to -4.2 eV in the hydride. The change in the Al bands on hydrogenation of Th_2Al is apparently associated with the electron transfer from Th to Al. The H-s bands are found in the energy range from -2 eV to the bottom of the VB, whereas their contribution at E_F is negligibly small indicating bands with more localized character. The bands at E_F are dominated by the Al-3p and Th-6d electrons in both Th_2Al and Th_2AlH_4. Owing to the creation of the pseudogap feature near E_F, the contributions of the Al-3p electrons to the bands at the E_F level are significantly reduced by the hydrogenation of Th_2Al.

E. Nature of chemical bonding

1. Density of states

In order to obtain a deeper insight into the changes in chemical bonding behavior on hydrogenation of Th_2Al we give the angular-momentum and site-decomposed density of states (DOS) for Th_2Al and Th_2AlH_4 in Fig. 6. DOS features for Th_2Al and Th_2AlH_4 show close similarity. Both exhibit metallic character since there is a finite DOS at E_F. From the DOS features we see that E_F is systematically shifted toward higher energy in Th_2AlH_4. This is due to the increase in the number of valence electrons when Th_2Al is hydrogenated. The DOS for both Th_2Al and Th_2AlH_4 lies mainly in four energy regions: (a) the lowest region around -20 eV stems mainly from localized or tightly bound Th-6p states, (b) the region from -9.25 to -2.5 eV originates from bonding of H-1s, Al-3p, and Th-6d (Al-3p and Th-6d states in Th_2Al), (c) the region from -2.5 to 0 eV comes from bonding states of Al-3p and Th-6d, and (d) the energy region just above E_F (0 to 3.5 eV) is dominated by unoccupied Th-4f states.

The semicore Th-6p states are well localized and naturally their effect on bonding is very small. On comparing the Th-6p DOS of Th_2Al and Th_2AlH_4, it is seen that the width is significantly reduced in Th_2AlH_4 owing to the lattice expansion and the inclusion of additional energy levels below E_F. In the VB region, the bandwidth and DOS are larger for Th_2AlH_4 than for Th_2Al. Hydrogenation enhances interaction between neighboring atoms, thereby increases the overlap of orbitals, and in turn results in the enlarged VB width in Th_2AlH_4. In particular, the strong hybridization between Th-6d and H-1s states increases the VB width from 7.1 eV in Th_2Al to 8.4 eV in Th_2AlH_4. H-1s, Al-3p, and Th-6d states are energetically degenerate in the VB region indicating a possibility of covalent Th-H, Th-Al, and Al-H bonds. However, the spatial separation of Th-Al (3.22 Å) and Al-H (3.02 Å) is larger than the Th-H separation (2.26 Å). Therefore, covalent bonds between the former pairs are small whereas there is a significant covalent contribution between Th and H. In conformity with this, the COHP and charge-density analyses show directional bonding between Th and H (see Secs. III E 2 and III E 3). The accommodation of H in the interstitial position between Th and Al creates new bonding states between Th and H. This also increases the Th-Al distance around 2.2% compared with that in Th_2Al. The consequence of this enhancement is that the Al DOS in the VB region becomes narrow and the splitting between the Al-3s and Al-3p states is almost doubled (see Fig. 6). The finite DOS at E_F which gives the metallic character of Th_2Al and Th_2AlH_4 comes from Th-d states in addition to some states of Al-p character.

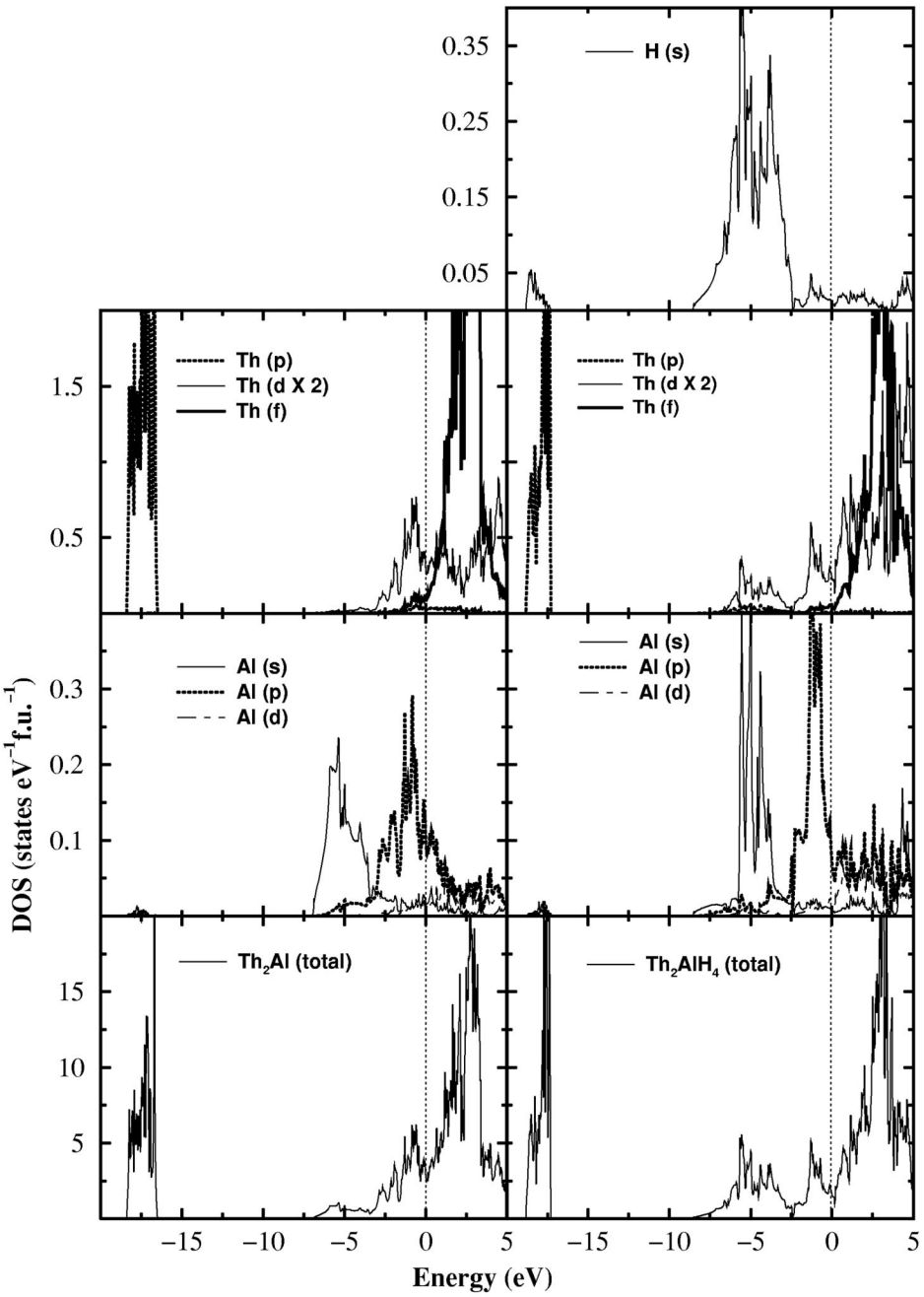

FIG. 6. Total, site, and orbital projected densities of states for (a) Th_2Al and (b) Th_2AlH_4.

Another interesting feature of the total DOS of Th_2AlH_4 is the presence of a deep valley around E_F which is termed as a pseudogap. Pseudogap features are formed not only in crystalline solids[35] but occur also in amorphous phases[36] and quasicrystals.[37] Two mechanisms have been proposed for the occurrence of pseudogaps in binary alloys, one attributed to ionic features and the other to the effect of hybridization. Although the electronegativity differences between Th, Al, and H are noticeable, they are not large enough to explain the pseudogap in Th_2AlH_4. Hence hybridization must be the cause for the creation of the pseudogap in Th_2AlH_4. There is also proposed a correlation between the occurrence of pseudogaps and structural stability,[38] in that materials which possess pseudogaps in the vicinity of E_F usually have higher stability. This correlates with the higher value of ΔH in Th_2AlH_4 than in Th_2Al (Table III).

2. Charge density

The analysis of the bonding between the constituents will give a better understanding about the anisotropic changes in the structural parameters on hydrogenation of Th_2Al. Figure 7 shows the calculated valence-charge density (obtained directly from the self-consistent calculations) within ab and ac planes for Th_2AlH_4. The Th, Al, and H atoms are confined to layers along c, with Th and Al being situated in alternating

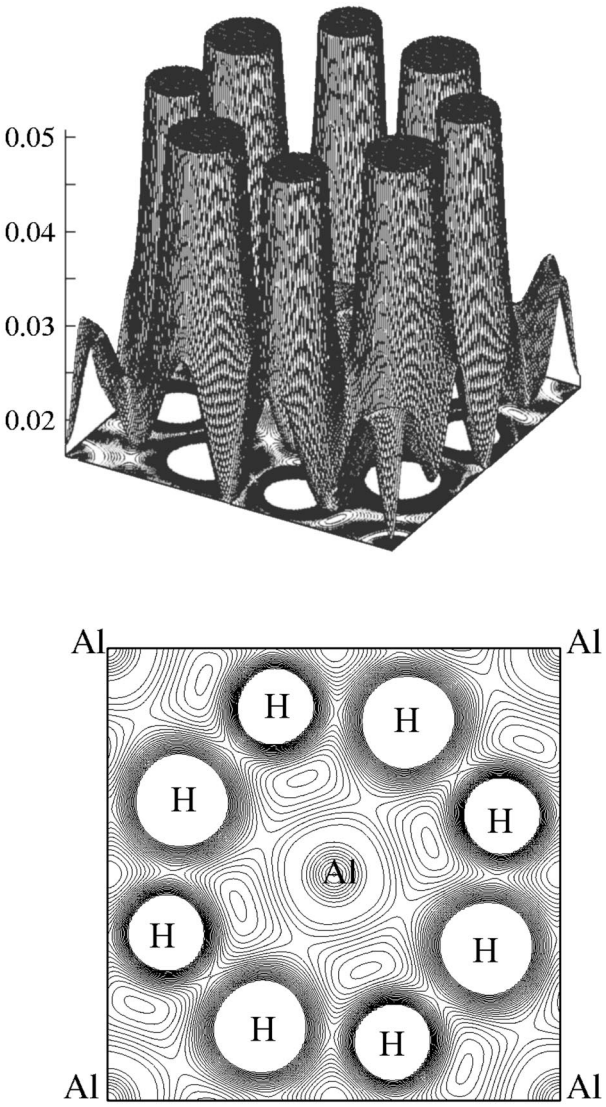

FIG. 7. Valence electron charge-density plot for Th_2AlH_4 in the *ab* plane (through H) with 40 contours drawn between 0 and 0.25 electrons/a.u.^{3}.

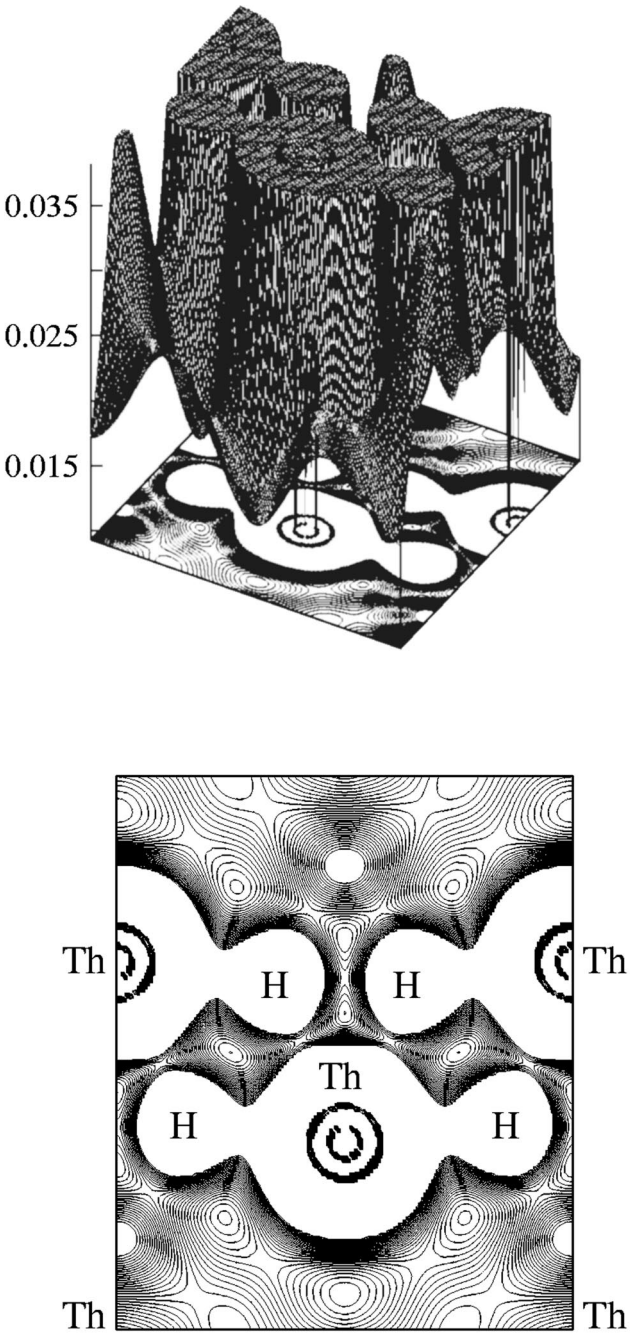

FIG. 8. Valence electron charge-density plot between the Th and H atoms for Th_2AlH_4 in the *ac* plane (through H)with 40 contours drawn between 0 and 0.25 electrons/a.u.^{3}.

metal layers with hydrogen in between, hence establishing a sequence of ···-Th-H-Al-H-Th-H-Al-H-Th-··· layers (see Fig. 1). The H atoms are arranged in a chainlike manner within the *ab* plane as also evident from Fig. 7 (lower figure). It is interesting to note that the nature of the H-H bonding is quite different along *a* and *c*. Although the H-H distance is 2.34 Å within the basal plane and 1.95 Å perpendicular to the basal plane, the bonding between the H atoms is not totally dominated by the covalent interactions along *c*. In fact, the COHP analyses (Sec. III E 3) shows that the covalent H-H interaction within the *ab* plane is larger than that within the *ac* plane. Examination of the partial DOS (PDOS) (see Fig. 6) shows that the valence electrons of Th and Al in Th_2Al are not energetically degenerate in the VB region and this indicates that there is a degree of ionic character in their bonding in line with their electronegative difference. When H is introduced to the Th_2Al lattice the PDOS value in the VB of Th is drastically reduced whereas the corresponding PDOS value in the VB of Al is increased. In conformity with this the integrated charge inside the Al sphere is around 0.59 electrons (0.8 electrons according to the TBLMTO method) larger in Th_2AlH_4 than in Th_2Al. This indicates that the ionic character of the bonding between Th and Al is increased on the hydrogenation of Th_2Al.

The bonding between Th and H is predominantly covalent as evidenced by the finite charge between these atoms (see Fig. 8). The H-*s* electrons are tightly bound to the Th-*d*

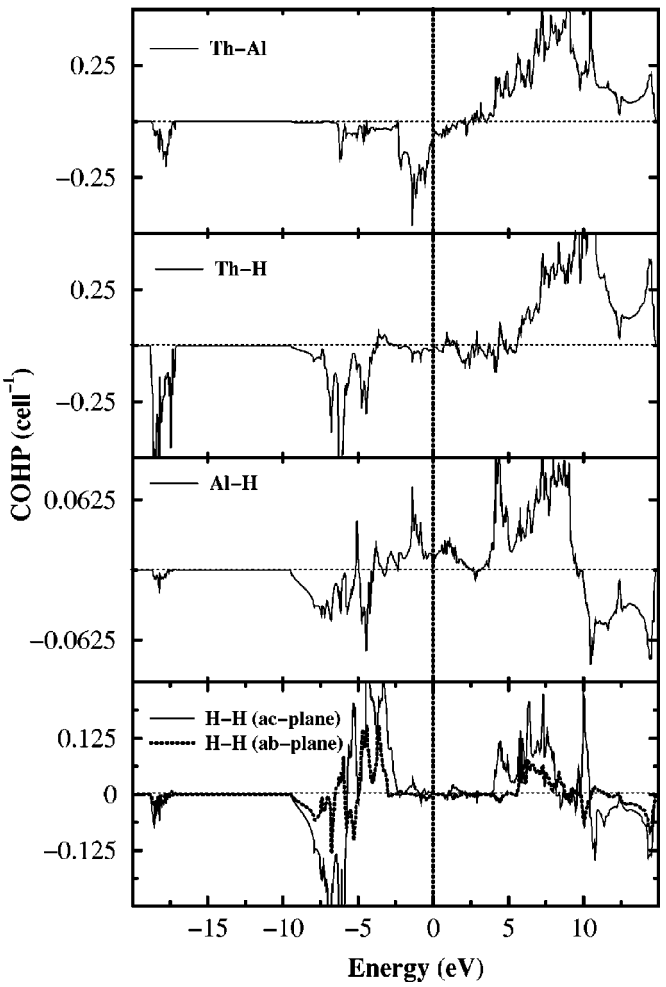

FIG. 9. COHP for Th_2AlH_4, depicting the contributions from Th-Al, Th-H, Al-H, and H-H interactions. The COHP for H atoms in the ab plane and ac plane are given as solid and dotted lines, respectively.

states, and the Th-H arrangement forms an H-Th-H dumbbell pattern. Now we will try to obtain a possible explanation for the short H-H distance within the ac plane of Th_2AlH_4 from the charge-density analysis. The strong covalent interaction between Th and H in the ac plane (see Fig. 8, lower part) and the dumbbell pattern tend to draw the electrons of H towards Th leaving only a small amount of electrons between the H along c to repel each other. The main reason for this short H-H distance is then a reduced repulsion rather than a bonding interaction between them.

3. COHP

The COHP is an extremely useful tool to analyze covalent bonding interaction between atoms, the simplest approach being to investigate the complete COHP between the atoms concerned, taking all valence orbitals into account. The COHP between Th-H, Th-Al, Al-H, and H-H in Th_2AlH_4 is given in Fig. 9.

Owing to the very different interatomic distances between the H atoms in the ab and ac planes, special attention is paid to the COHP in these planes. Both bonding and antibonding states are present almost equally in the VB region indicating that covalent interaction between the H atoms is not participating significantly in the stability of Th_2AlH_4. On the other hand, the bonding states are present in the whole VB region in the COHP of Th-Al and Th-H indicating that covalent interaction between these pairs is contributing to structural stability. The presence of the large bonding states in the VB region of the COHP for Th-H along with the enhancement of the ionic bonding between Th and Al on hydrogenation comply with the larger value of heat of formation for Th_2AlH_4 compared with Th_2Al. In order to quantify the covalent interaction between the constituents of Th_2AlH_4 we have integrated the COHP curves up to E_F for Th-Al, Th-H, and Al-H giving -0.778, -1.244, and -0.072 eV, respectively. Owing to the presence of both bonding and antibonding states below E_F in the COHP the integrated value for H-H becomes negligibly small (-0.086 and -0.011 eV within the ac and ab planes, respectively, but as the integrated value of bonding states alone is -0.571 and -0.136 eV, respectively, the bonding H-H interaction is quite different in the two planes). Hence, one can conclude that the bond strength between the constituents of Th_2AlH_4 decreases in the order Th-H>Th-Al>Al-H>H-H.

The experimental[5,9] and theoretical studies show highly anisotropic changes in the lattice expansion on hydrogenation of Th_2Al. According to the crystal structure of Th_2Al the interatomic distance between the interstitial regions where one can accommodate H in the ab plane is $\sim$2.4 Å. Hence, there is a large flexible space for accommodation of the H atoms in this plane without the need to expand the lattice. In contrast, the interatomic distance between the interstitial regions in the ac plane is only $\sim$1.65 Å. So, large expansion of the lattice along c is necessary to accommodate H within the ac plane. As a result, even with a short H-H separation of 1.95 Å, a volume expansion of 12.41% is needed when Th_2AlH_4 is formed from Th_2Al. The experimental observation of 0.105% lattice expansion along a and 12.15% along c is found to be in excellent agreement with the theoretically obtained values of 0.03% and 12.41%, respectively.

IV. CONCLUSION

This study reports a detailed investigation on the electronic structure, bonding nature, and ground-state properties of Th_2Al and Th_2AlH_4 using first-principles methods. The following important conclusions are obtained.

(1) The calculations show that Th_2Al and Th_2AlH_4 are ''formed'' in the $CuAl_2$-type crystal structure; the optimized atomic positions and lattice parameters are in very good agreement with recent experimental results.

(2) Structural optimization gives the shortest H-H separation of 1.95 Å, which is close to the recent experimental value of 1.97 Å.

(3) We observed a highly anisotropic volume expansion of 12.47% of the Th_2Al matrix on hydrogenation to Th_2AlH_4, of which 99.76% occurs perpendicular to the basal plane.

(4) The large difference in interatomic distance between the interstitial regions within the ab and ac planes and the strong covalent interaction between Th and H along c keep

the H atoms close together in the *c* direction. These are the main reasons for the highly anisotropic volume expansion on hydrogenation of Th_2Al.

(5) Charge-density and COHP analyses reveal that the Th-H bonds are stronger than the H-H bonds and other localized bonds in this structure. The formation of strongly bonded ThH_2 subunits in Th_2AlH_4 makes the repulsive interaction between the H atoms smaller along *c* and this is the precise reason for the violation of the 2-Å rule.

(6) There appears to be a correlation between c/a and the structural stability of hydrated $CuAl_2$-type phases. For phases with $c/a<0.825$, the symmetry changes from $I4/mcm$ to $P4/ncc$ on hydrogenation, whereas for $c/a>0.825$, the crystal symmetry is not affected on hydrogenation.

(7) Density-of-states and band-structure studies show that Th_2Al and Th_2AlH_4 have nonvanishing $N(E_F)$, resulting in metallic character. The cohesive energy analysis shows that Th_2AlH_4 is more stable than Th_2Al.

ACKNOWLEDGMENTS

P.V. gratefully acknowledges Professor Karlheinz Schwarz, Professor Peter Blaha, Professor O.K. Andersen, and Professor O. Jepsen for supplying computer codes used in this study. The authors also acknowledge Dr. Florent Boucher for useful discussions on the COHP. This work has received support from The Research Council of Norway (Program for Supercomputing) through a grant of computing time.

*Electronic address: ponniah.vajeeston@kjemi.uio.no

[1] B.K. Rao and P. Jena, Phys. Rev. B **31**, 6726 (1985).
[2] D.G. Westlake, J. Less-Common Met. **103**, 203 (1984).
[3] C. Switendick, Z. Phys. Chem., Neue Folge **117**, 89 (1979).
[4] K. Yvon and P. Fischer, in *Hydrogen in Intermetallic Compounds*, Springer Series in Topics in Applied Physics, Vol. 63, edited by L. Schlapbach, (Springer, Berlin, 1988), p. 87.
[5] J. Bergsma, J.A. Goedkoop, and J.H.N. van Vucht, Acta Crystallogr. **14**, 223 (1961).
[6] S.C. Abrahams, A.P. Ginsberg, and K. Knox, Inorg. Chem. **3**, 558 (1964); K. Knox and A.P. Ginsberg, *ibid.* **3**, 555 (1964).
[7] E.E. Havinga, H. Damsama, and P. Hokkeling, J. Less-Common Met. **27**, 169 (1972).
[8] V.A. Yartys, H. Fjellvåg, B.C. Hauback, and A.B. Riabov, J. Alloys Compd. **274**, 217 (1998).
[9] M.H. Sørby, H. Fjellvåg, B.C. Hauback, A.J. Maeland, and V.A. Yartys, J. Alloys Compd. **309**, 154 (2000).
[10] A. Chikdene, A. Baudry, P. Boyer, S. Miraglia, D. Fruchart, and J.L. Soubeyroux, Z. Phys. Chem., Neue Folge **163**, 219 (1989).
[11] H. Nakamura, D. Nguyen-Manh, and D.G. Pettifor, J. Alloys Compd. **281**, 81 (1998).
[12] J.J. Murray, M.L. Post, and J.B. Taylor, J. Less-Common Met. **80**, 211 (1981).
[13] B.S. Bowerman, C.A. Wulf, and T.B. Flanagan, Z. Phys. Chem. (Munich) **116**, 197 (1979).
[14] W.N. Hubbard, P.L. Rawlins, P.A. Connick, R.E. Stedwell, and P.A.G.O. Hare, J. Chem. Thermodyn. **13**, 785 (1983).
[15] F. Boucher and R. Rousseau, Inorg. Chem. **37**, 2351 (1998).
[16] R. Dronskowski and P.E. Blochl, J. Phys. Chem. **97**, 8617 (1993).
[17] P. Villars and L.D. Calvert, *Pearson's Handbook of Crystallographic Data for Intermetallic Phases*, 2nd ed. (American Society for Metals, Metals Park, OH), Vol. 3.
[18] P. Blaha, K. Schwarz, and J. Luitz, COMPUTER CODE WIEN97 (Vienna University of Technology, Vienna, Austria, 1997); Comput. Phys. Commun. **59**, 399 (1990).
[19] D. Singh, *Plane Waves, Pseudopotentials, and the LAPW Method* (Kluwer Academic, New York, 1994).
[20] J.P. Perdew, in *Electronic Structure of Solids*, edited by P. Ziesche and H. Eschrig (Akademie Verlag, Berlin, 1991), p. 11; J.P. Perdew, K. Burke, and Y. Wang, Phys. Rev. B **54**, 16 533 (1996); J.P. Perdew, K. Burke, and M. Ernzerhof, Phys. Rev. Lett. **77**, 3865 (1996).
[21] D. Singh, Phys. Rev. B **43**, 6388 (1991).
[22] P.E. Blochl, O. Jepsen, and O.K. Andersen, Phys. Rev. B **49**, 16 223 (1994).
[23] O.K. Andersen, Phys. Rev. B **12**, 3060 (1975); O.K. Andersen, and O. Jepsen, Phys. Rev. Lett. **53**, 2571 (1984); H. L. Skriver, *The LMTO Method* (Springer, Heidelberg, 1984).
[24] G. Krier, O. Jepsen, A. Burkhardt, and O.K. Andersen, TIGHT BINDING LMTO-ASA PROGRAM, Version 4.7 (Stuttgart, Germany, 2000).
[25] P. Ravindran, G. Subramoniam, and R. Asokamani, Phys. Rev. B **53**, 1129 (1996).
[26] C. Ravi, P. Vajeeston, S. Mathijaya, and R. Asokamani, Phys. Rev. B **60**, 15 683 (1999).
[27] P. Vajeeston, P. Ravindran, C. Ravi, and R. Asokamani, Phys. Rev. B **63**, 045115 (2001).
[28] D.C. Patton, D.V. Porezag, and M.R. Pederson, Phys. Rev. B **55**, 7454 (1999).
[29] H.H. Van Mal, K.H. Buschow, and A.R. Miedema, J. Less-Common Met. **35**, 65 (1973).
[30] P. Vinet, J.H. Rose, J. Ferrante, and J.R. Smith, J. Phys.: Condens. Matter **1**, 1941 (1989).
[31] J. Osterwalder, T. Riesterer, L. Schlapbach, F. Vaillant, and D. Fruchart, Phys. Rev. B **31**, 8311 (1985).
[32] L. Schlapbach, F. Meli, and A. Zuttel, *in Intermetallic Compounds*, edited by J. H. Westbrook and R. L. Fleischer (Wiley, New York, 1994), Vol. 2, Chap. 21, pp. 475–488.
[33] F. Bonhomme, K. Yvon, and M. Zolliker, J. Alloys Compd. **199**, 129 (1993).
[34] M.M. Elcombe, S.J. Campbell, C.J. Howard, H.G. Buttner, and F. Aubertin, J. Alloys Compd. **232**, 174 (1999).
[35] J.H. Xu and A.J. Freeman, Phys. Rev. B **41**, 12 553 (1990).
[36] A. Pasturel, C. Colinet, and P. Hicter, Physica B & C **132**, 177 (1985).
[37] J.C. Phillips, Phys. Rev. B **47**, 2522 (1992).
[38] P. Ravindran and R. Asokamani, Bull. Mater. Sci. **20**, 613 (1997); V.L. Moruzzi, P. Oelhafen, and A.R. Williams, Phys. Rev. B **27**, 7194 (1983).